ACS Infectious Diseases

Article

Cite This: ACS Infect. Dis. XXXX, XXX, XXX−XXX

pubs.acs.org/journal/aidcbc

Avoiding Antibiotic Inactivation in *Mycobacterium tuberculosis* by Rv3406 through Strategic Nucleoside Modification

Matthew R. Bockman,[†] Curtis A. Engelhart,[‡] Surendra Dawadi,[†] Peter Larson,[†] Divya Tiwari,[‡] David M. Ferguson,[†] Dirk Schnappinger,[‡] and Courtney C. Aldrich*,[†]

[†]Department of Medicinal Chemistry, University of Minnesota, 308 Harvard Street SE, Minneapolis, Minnesota 55455, United States

[‡]Department of Microbiology and Immunology, Weill Cornell Medical College, 1300 York Avenue, New York, New York 10021, United States

Supporting Information

ABSTRACT: 5′-[*N*-(D-biotinoyl)sulfamoyl]amino-5′-deoxyadenosine (Bio-AMS, **1**) possesses selective activity against *Mycobacterium tuberculosis* (*Mtb*) and arrests fatty acid and lipid biosynthesis through inhibition of the *Mycobacterium tuberculosis* biotin protein ligase (*Mt*BPL). *Mtb* develops spontaneous resistance to **1** with a frequency of at least 1×10^{-7} by overexpression of Rv3406, a type II sulfatase that enzymatically inactivates **1**. In an effort to circumvent this resistance mechanism, we describe herein strategic modification of the nucleoside at the 5′-position to prevent enzymatic inactivation. The new analogues retained subnanomolar potency to *Mt*BPL (K_D = 0.66−0.97 nM), and 5′*R*-*C*-methyl derivative **6** exhibited identical antimycobacterial activity toward: *Mtb* H37Rv, *Mt*BPL overexpression, and an isogenic Rv3406 overexpression strain (minimum inhibitory concentration, MIC = 1.56 μM). Moreover, **6** was not metabolized by recombinant Rv3406 and resistant mutants to **6** could not be isolated (frequency of resistance <1.4×10^{-10}) demonstrating it successfully overcame Rv3406-mediated resistance.

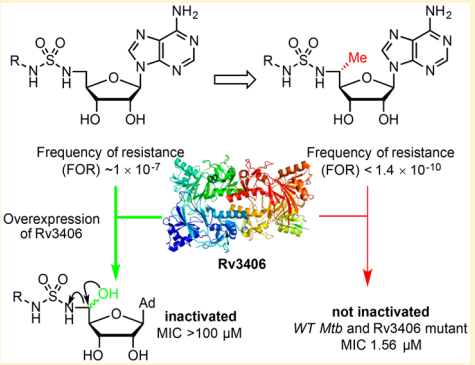

KEYWORDS: *biotin protein ligase, Mycobacterium tuberculosis, tuberculosis, metabolism, adenylation, bisubstrate inhibitor*

Despite great advances in human medicine over the last century, tuberculosis (TB), caused by *Mycobacterium tuberculosis* (*Mtb*), remains a global health problem.[1] In 2015, TB overtook HIV as the leading source of infectious disease mortality worldwide. Treatment of simple drug-susceptible TB is very challenging, compared to most bacterial infections, requiring 6−9 months of a four-drug regimen comprised of isoniazid, rifampicin, ethambutol, and pyrazinamide. These drugs were discovered over 40 years ago and remain the cornerstone of TB chemotherapy. The underlying origin of the persistence and drug tolerance of *Mtb in vivo* that necessitates this long treatment course is still not fully understood but is likely multifactorial. Considering the unique challenges posed by drug susceptible TB, the emergence and dissemination of multidrug resistant TB (MDR-TB) and extensively drug resistant TB (XDR-TB), which are minimally resistant to the two most effective antitubercular agents, isoniazid and rifampicin, are a global health crisis.

Mycobacteria produce a tremendously diverse array of lipophilic molecules ranging from simple short-chain fatty acids to the very long-chained mycolic acids.[2,3] The mycolic acids are essential components of the mycobacterial cell envelope where they shield the bacterium from host-induced oxidative stress and contribute to intrinsic drug resistance.[4] Other lipids such as phthiocerol dimycocerosates (PDIMs), phenolic glycolipids, and trehalose dimycolates limit innate immune responses by complementary mechanisms while glycolipids and lipoproteins have been implicated in modulating adaptive immunity.[5−7] Fatty acid degradation is also believed to be important, and several lines of evidence support the hypothesis that mycobacteria are primarily lipolytic *in vivo*, deriving sugars needed for nucleotide and cell wall biosynthesis by breakdown of host fatty acids via gluconeogenesis.[8] Biotin protein ligase (BPL) in *Mtb* represents an extremely attractive metabolic target since it globally regulates lipid metabolism through the post-translational biotinylation of the three nonredundant acyl CoA carboxylases (ACC1, ACC2, and ACC3) involved in the synthesis of different malonyl coenzyme A (CoA) building blocks used in mycobacterial lipid synthesis as well as pyruvate CoA carboxylase, which catalyzes the first step in gluconeogenesis.[9−11] Genetic silencing of *Mycobacterium tuberculosis* biotin protein ligase (*Mt*BPL) eliminated *Mtb* from mice during both acute and chronic infections demonstrating *Mt*BPL's essential role in *Mtb* survival and persistence.[12] Moreover, partial genetic inactivation of *Mtb*'s ability to synthesize biotin was found to significantly enhance clearance of *Mtb* from lungs and spleen by rifampicin serving to validate *Mt*BPL as a vulnerable target.[12]

Received: February 10, 2018

DOI: 10.1021/acsinfecdis.8b00038
ACS Infect. Dis. XXXX, XXX, XXX−XXX

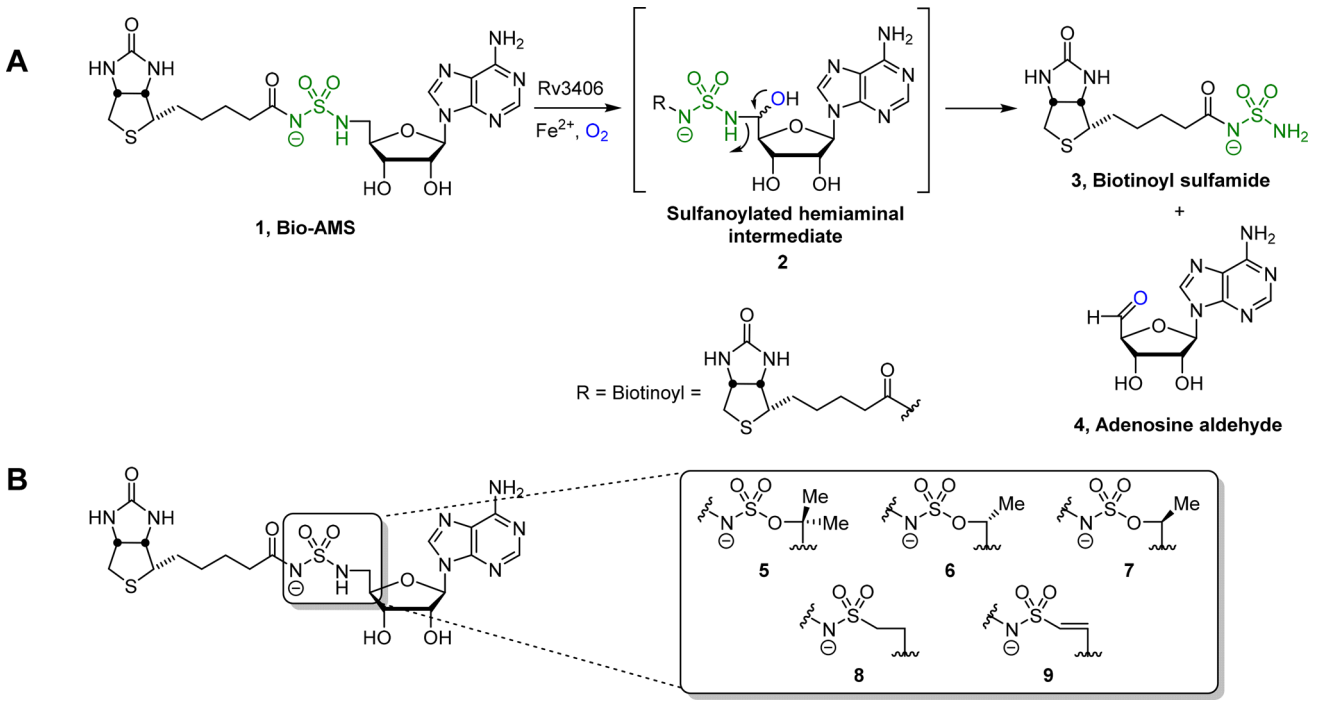

Figure 1. (A) Rv3406-mediated inactivation of Bio-AMS. (B) Proposed analogues to overcome metabolism by Rv3406.

Bisubstrate inhibitors have been described for the structurally related BPL from *Staphylococcus aureus* including alkylphosphates,[13] β-ketophosphonates,[14] and triazole nucleosides,[15,16] as well as analogues wherein the adenosine nucleobase was replaced with benzoxazoline[17,18] and aryl moieties.[19] We have reported 5′-[*N*-(D-biotinoyl)sulfamoyl]amino-5′-deoxyadenosine (Bio-AMS, **1**, Figure 1A) is a potent subnanomolar bisubstrate inhibitor of the mycobacterial biotin protein ligase (*Mt*BPL).[20] Bio-AMS possesses excellent antitubercular activity against *Mtb* H37Rv and MDR/XDR-TB strains with minimum inhibitory concentrations (MICs) ranging from 0.16 to 0.625 μM and is not affected by changes to the primary carbon source.[12,20−22] Bio-AMS also has potent bactericidal activity similar to isoniazid and sterilized an *Mtb* culture of 5×10^6 colony forming units (CFU) within 3 weeks.[12] Tiwari, Schnappinger, and co-workers recently demonstrated the most frequent mechanism of Bio-AMS resistance is caused by overexpression of Rv3406, a type II sulfatase involved in the scavenging of inorganic sulfates for metabolic and biosynthetic purposes.[22] Rv3406 was shown to oxidize the 5′-methylene carbon of Bio-AMS to hemiaminal **2**, which disproportionates into biotinoyl sulfamide **3** and adenosine 5′-aldehyde **4** (Figure 1A). Herein, we report the synthesis and biochemical and biological evaluation of four Bio-AMS analogues designed to circumvent Rv3406-mediated chemical inactivation. Our first series of analogues sterically block oxidation by incorporation of methyl groups at the 5′-*C* position of Bio-AMS (**5**−**7**, Figure 1B) while our second set of compounds were conceived to prevent disproportionation through replacement of the 5′-amino group in Bio-AMS with a carbon atom (**8**, **9**, Figure 1B).

RESULTS

Our initial strategy focused on the synthesis of a 5′-gem-dimethyl analogue of **1** lacking a C5′-hydrogen atom and thus intrinsically resistant to Rv3406 metabolism. The synthesis began by (2,2,6,6-tetramethylpiperidin-1-yl)oxyl (TEMPO) oxidation of commercially available 2′,3′-*O*-isopropylideneadenosine **10** to give carboxylate **11**,[24] which was converted to 5′-methyl ester **12** with diazomethane (Scheme 1).[25] Grignard

Scheme 1. Synthesis of 5′-*C*,*C*-Dimethyladenosine

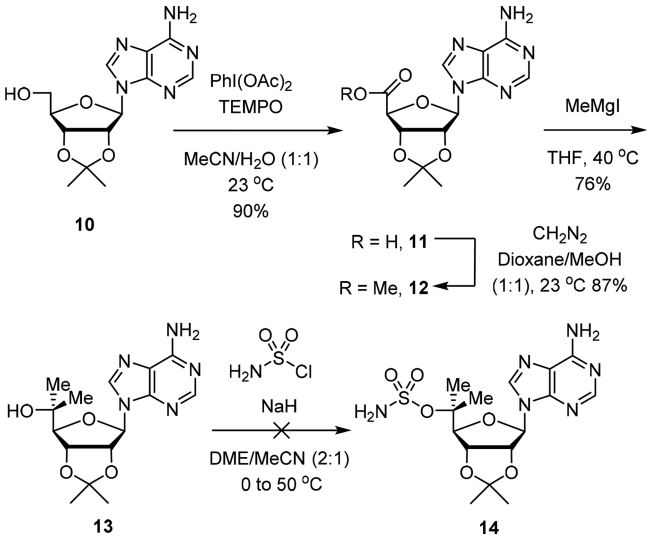

addition to **12** using methylmagnesium iodide at 40 °C afforded 5′-*C*,*C*-dimethyl adenosine **13**. Unfortunately, sulfamoylation of the tertiary alcohol under a variety of conditions led to either no reaction or β-elimination (Table S3).[26]

We therefore opted to incorporate a single methyl group at the 5′ position, which introduces a stereocenter, but we expected may be sufficient to sterically block Rv3406-mediated oxidation while not being susceptible to the undesired β-elimination observed with tertiary alcohol **13**. The 5′*R*-*C*-methyl and 5′*S*-*C*-methyl analogues of **1** were conveniently synthesized employing an asymmetric transfer hydrogenation (ATH) reaction developed by Bligh and co-workers.[27]

DOI: 10.1021/acsinfecdis.8b00038
ACS Infect. Dis. XXXX, XXX, XXX−XXX

Reduction of ketone **16** with chloro{[(1*R*,2*R*)-(−)-2-amino-1,2-diphenylethyl](4-toluenesulfonyl)amido}(*p*-cymene)-ruthenium(II) ((*R*,*R*)-TsDPEN) and chloro{[(1*S*,2*S*)-(−)-2-amino-1,2-diphenylethyl](4-toluenesulfonyl)amido}(*p*-cymene)ruthenium(II) ((*S*,*S*)-TsDPEN) catalysts afforded 5′*R*-*C*-methyl **17** and 5′*S*-*C*-methyl **18**, respectively (Scheme 2).[27]

Scheme 2. Synthesis of Both 5′*R*-*C*-Methyl-BioAMS (6) and 5′*S*-*C*-Methyl-BioAMS (7) Analogues

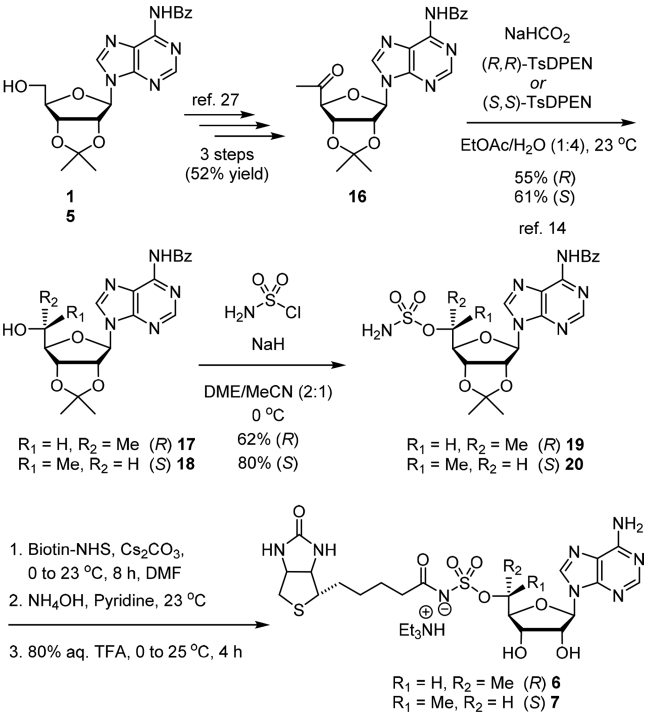

Both reactions yielded the secondary alcohols in 99% diastereomeric purity, as confirmed by reverse-phase high performance liquid chromatography (HPLC) analysis and comparison to the reported ^{1}H NMR spectra.[27] Optimization of our previously described sulfamoylation conditions[28] using sodium hydride as the base and freshly synthesized sulfamoyl chloride in a 2:1 mixture of 1,2-dimethoxyethane (DME) and acetonitrile provided 5′*R*-*C*-methyl **19** and 5′*S*-*C*-methyl **20** (Scheme 2). Biotinylation of sulfamates **19** and **20** employing D-(+)-biotin *N*-hydroxysuccinimide ester (Biotin-NHS) mediated by cesium carbonate furnished the corresponding biotinylated adducts, which were sequentially deprotected using saturated aqueous ammonia and 80% aqueous trifluoroacetic acid (TFA) to remove the *N*-benzoyl and isopropylidene groups. Preparative reverse-phase HPLC purification afforded the final biotinylated analogues **6** and **7** as the triethylammonium salts in 33% and 22% yields, respectively, over the final three steps. Both **6** and **7** were stable due to the increased steric bulk at C-5′ and did not undergo cyclonucleoside formation through nucleophilic attack of the N3 adenine atom onto C-5′, which we have observed is a major decomposition pathway for the corresponding nonmethylated sulfamate analogue (wherein $R^1 = R^2 = H$).[20,21] Bio-AMS avoids cyclonucleoside formation by virtue of the poor nucleofugacity of the sulfamide compared to the sulfamate at C-5′.

The synthesis of sulfonamide analogue **8** has been reported in our previous work.[20,21] The vinyl sulfonamide **9** was synthesized in an analogous route avoiding the hydrogenation step, starting from protected nucleoside **21** in a two-step one-pot procedure through oxidation and subsequent Horner-Wittig olefination using *N*-Boc-diphenylphosphorylmethanesulfonamide to provide **22**. Chemoselective deprotection of the three *tert*-butyloxycarbonyl (Boc) protecting groups in the presence of the isopropylidene was accomplished with 20% TFA in CH_2Cl_2 to yield the vinyl sulfonamide **23**.[21] Biotinylation and deprotection furnished **9** (Scheme 3).[21]

Scheme 3. Synthesis of Vinyl Sulfonamide Bio-AMS (9) Analogue

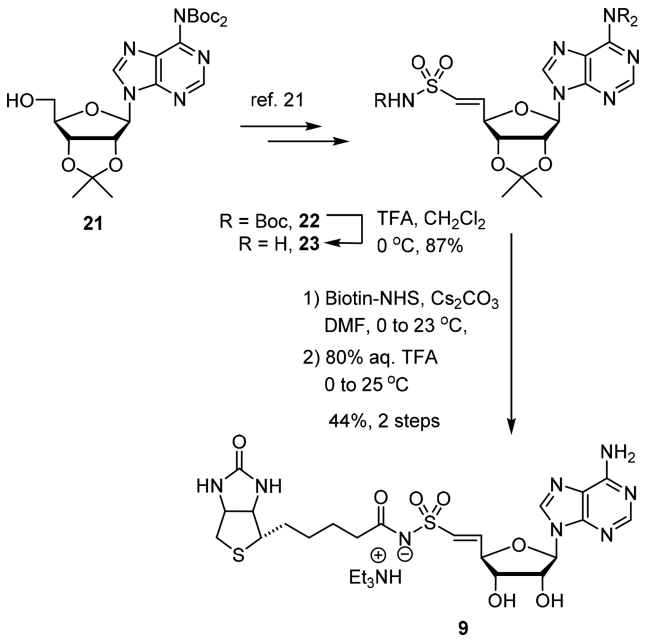

Each of the inhibitors was evaluated by isothermal titration calorimetry (ITC) in a direct titration experiment with *Mt*BPL. However, the binding affinity was too high to determine, and we simply observed stoichiometric titration of the protein. We thus employed displacement ITC experiments, in which the ligands were titrated into a solution of *Mt*BPL prebound to biotin to measure the apparent dissociation constants.[29] The true dissociation constants (K_D) were subsequently determined as described in the experimental section. The K_D values of **6**−**9** were nearly identical ranging from 0.66 to 0.97 nM (Table 1). The results were further evaluated using the X-ray cocrystal structure of **1** in *Mt*BPL (PDB: 3rux). Model building techniques were applied to examine the fit of the added methyl groups of **6** and **7** within the active site of *Mt*BPL (Figure S6). The model shows the 5′-C-methyl groups project toward Arg72 and Gly73 of an exterior loop region (Arg67−Ala75). Given the experimental binding affinities of **1**, **6**, and **7** are nearly equivalent, it is fair to conclude that these potential contacts have a minimal impact on ligand binding affinity, which presumably is a result of the inherent flexibility of the exterior loops.

The whole-cell antitubercular activity of each compound was evaluated against wild-type (WT) *Mtb* (H37Rv), two *Mtb* strains which overexpress *Mt*BPL to different degrees (hereafter referred to as *Mt*BPL-H and *Mt*BPL-M, described in our previous work, Figure 2),[20] and a *Mtb* mutant that highly overexpresses Rv3406 (hereafter referred to as Rv3406-overexpressor or Rv3406-OE). The parent compound **1** was

DOI: 10.1021/acsinfecdis.8b00038
ACS Infect. Dis. XXXX, XXX, XXX−XXX

Table 1. MIC_{90} and Binding Data for Analogues 6–9

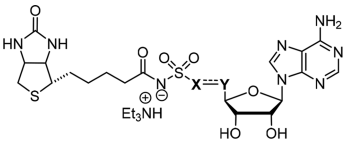

Compound		K_D, nM[a]	MIC_{90} (WT), μM[b]	MIC_{90} (Rv3406-OE), μM[c]	Frequency of Resistance[d]
1	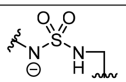	0.865	0.78	>100	$(0.1–4) \times 10^{-6}$
6	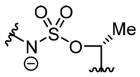	0.661	1.56	1.56	$< 1.4 \times 10^{-10}$
7	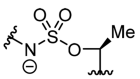	0.657	6.25	6.25	n.d.[e]
8	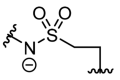	0.798	6.25	6.25	n.d.[e]
9	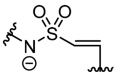	0.969	6.25	>100	n.d.[e]

[a]Competitive and direct ITC experiments to determine K_D and ΔG were performed in triplicate. All analogues possessed n values of 1.0 ± 0.2. The standard error of the K_D was ≤6.7% of the mean. [b]Minimum inhibitory concentrations (MIC) resulting in >90% growth inhibition of *M. tuberculosis* H37Rv. [c]MIC resulting in >90% growth inhibition of *M. tuberculosis* Rv3406-OE. Experiments were performed twice independently in triplicate. The MIC is defined as the lowest concentration of inhibitors that prevented growth, as determined by measuring the end point OD_{580} values. [d]Based on a concentration ten times the agar MIC of the compound tested. Approximately 10^8 cells were plated for **1** and 7×10^9 cells for **6**. FOR was calculated as the number of counted CFUs divided by the total number of bacteria plated. [e]Not determined.

active against WT *Mtb* possessing a MIC of 0.78 μM, but the MIC increased more than 125-fold to >100 μM against Rv3406-OE (Table 1). Compounds **1** and **6** showed a decrease in the susceptibility of *Mtb* by more than 125-fold when *Mt*BPL was overexpressed at both moderate (*Mt*BPL-M) and high levels (*Mt*BPL-H), demonstrating **1** and **6** both engage with *Mt*BPL in *Mtb* (Figure 2B,C). Consistent with their binding affinity to *Mt*BPL, analogues **6–9** maintained activity toward WT *Mtb*, yet the MICs were reduced 2–8-fold relative to **1**. 5′*R*-*C*-Methyl **6** was the most potent analogue examined against WT *Mtb* having a MIC of 1.56 μM. Remarkably, Rv3406-OE was equally sensitive to **6** indicating introduction of the 5′*R* methyl group fully overcame Rv3406-mediated resistance. The activities of diastereomeric analogue 5′*S*-*C*-methyl **7** and sulfonamide **8** both decreased 8-fold in potency relative to **1** and, similar to **6**, were equally active against WT *Mtb* and Rv3406-OE. We have shown that subtle changes to the ribose moiety of Bio-AMS resulted in decreased mycobacterial accumulation,[22] and we similarly expect the reduced activities of **7** and **8** may also be due to this phenomena. Among the four analogues studied, only vinyl sulfonamide **9** was inactive against Rv3406-OE. Additionally, to verify these compounds overcame Rv3406-mediated resistance, we attempted to isolate resistant mutants to **6** by plating 7×10^9 colony forming units (CFU) of *Mtb* on agar plates containing concentrations of **6** at 4- and 10-fold its agar MIC. We were unable to detect any colony growth after 9 weeks, indicating the frequency of resistance (FOR) for **6** is less than 1.4×10^{-10} at both 4- and 10-fold its agar MIC.

To biochemically verify the whole-cell results, each of the analogues were incubated with 3 μM recombinant Rv3406 as described[12] and the parent molecules and potential metabolites were analyzed by liquid chromatography tandem mass spectrometry (LC-MS/MS). Under these conditions, the time-dependent formation of **3** was readily observed. Rv3406 did not metabolize analogues **6–8**. For **6** and **7**, oxidation at the 5′ position was expected to provide the breakdown products *N*-biotinoylsulfamic acid (**S3**) and 5′-adenosine-methyl ketone (**S4**); however, neither of these were detected using authentic standards of the metabolites (Scheme S1). Rv3406 catalyzed oxidation of **8** was anticipated to produce a 5′-hydroxylsulfonamide Bio-AMS derivative (**S5**, Scheme S2) incapable of disproportionation, but a metabolite relating to an M + 16 peak was not identified. Compound **9** was the only analogue that we expected could undergo oxidation. Indeed, incubation of **9** with Rv3406 resulted in a time-dependent formation of an M + 16 metabolite tentatively assigned as epoxide **S6** (Figure S3). Rv3406 is a nonheme α-ketoglutarate-dependent Fe(II) dioxygenase, and epoxidation by the Fe(IV)=O active species is highly plausible based on the established chemistry of these enzymes.[30,31] Unfortunately, we were unable to isolate the metabolite **S6** or synthesize an authentic standard. We hypothesize epoxide ring-opening via nucleophilic water in solution forming a sulfamoylated diol, **S10**, which could then spontaneously decompose into *N*-biotinoylsulfuramidous acid (**S7**) and 5′-*C*-formyladenosine (**S8**) (Scheme S3B).

DISCUSSION

When examining *Mtb* clones resistant to **1**, there was no mutation in the target gene *birA* or to the promoter region.[12] Rather, the gene mutated in all resistant clones was *rv3405c*,

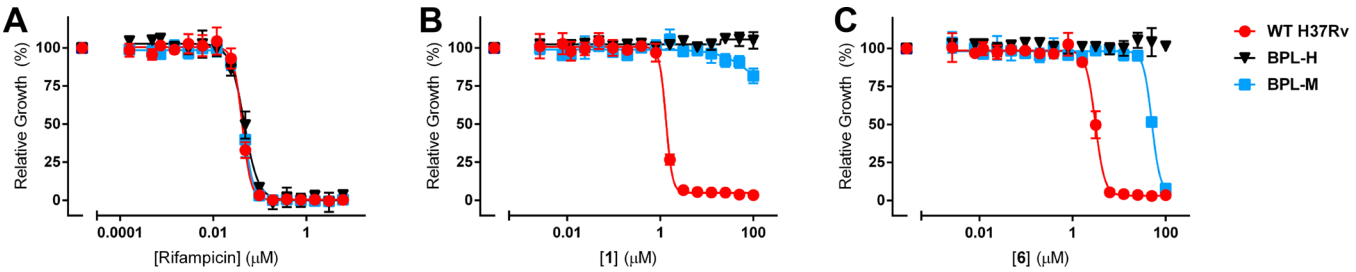

Figure 2. Susceptibility of *Mtb* [H37Rv (red circles), *Mt*BPL-H (black triangles), and *Mt*BPL-M (blue squares)] to (A) rifampicin (control), (B) Bio-AMS (**1**), and (C) 5′*R*-*C*-methyl-Bio-AMS (**6**). Normalized growth was calculated as OD_{580} at the indicated concentration divided by OD_{580} without drug (DMSO). Experiments were run in triplicate.

DOI: 10.1021/acsinfecdis.8b00038
ACS Infect. Dis. XXXX, XXX, XXX–XXX

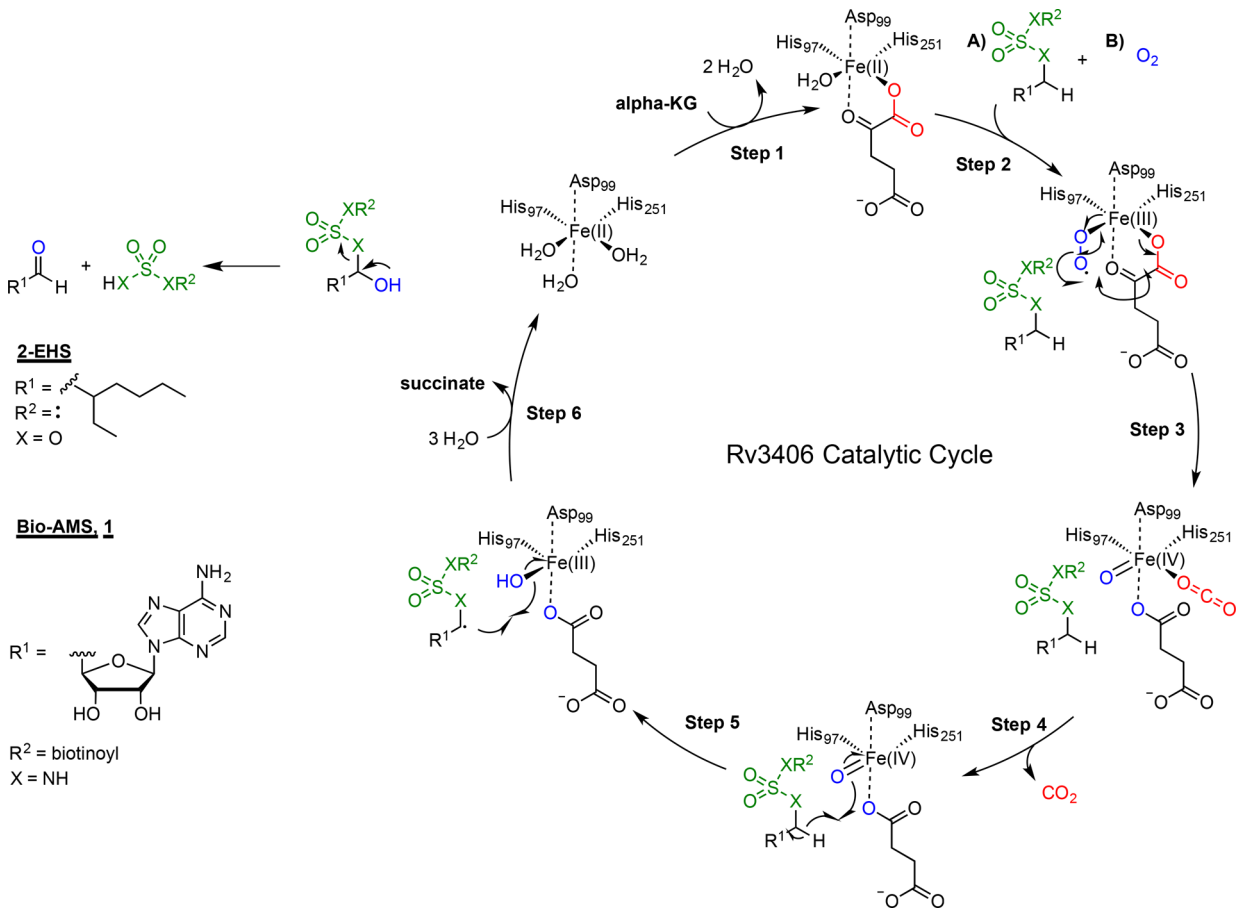

Figure 3. Proposed mechanism of Rv3406-mediate inactivation of **1**. (Step 1) A molecule of α-ketoglutarate (α-KG) binds to the iron, displacing two water molecules in the coordination sphere. (Step 2A) Substrate binds in the active site. (Step 2B) Substrate binding facilitates the coordination of oxygen to the iron. (Step 3) A tandem oxidation/decarboxylation of the iron/α-KG occurs, respectively, forming a ferryl Fe(IV)═O species. (Step 4) CO_2 dissociates from the iron core, allowing for the highly reactive ferryl species to abstract a hydrogen atom from the substrate. (Step 5) The ferryl Fe(IV)═O species is consequently reduced to Fe(III). The alkyl radical reacts further with the iron species through hydroxyl radical transfer, forming the sulfated hemiacetal or sulfamoylated hemiaminal intermediate and further reducing the iron core to Fe(II). (Step 6) Succinate is displaced from the iron center by three water molecules. The sulfated hemiacetal or sulfamoylated hemiaminal intermediate dissociates (bold arrow) and undergoes spontaneous disproportionation, affording an alkyl aldehyde and sulfate/sulfamide.

which is a member of the tetR family of DNA binding proteins. Rv3405c and the orthologous protein in *M. bovis* have been biochemically and biophysically characterized and shown to bind to the intergenic region between *rv3405c* and *rv3406* leading to their repression.[32,33] Indeed, we observed the mRNA levels of *rv3405c* and *rv3406* in the resistant isolates increased 10- and 190-fold, respectively.[12] The Rv3406-OE strain (used in this study) was constructed with an overexpression plasmid (pGMEH-Ptb38-rv3406) and found to have more than a 128-fold increase in MIC to **1**. Collectively, these data provide strong evidence for the overexpression of Rv3406 as the mechanism of resistance to **1**.

Rv3406 is a type II alkyl sulfatase. Currently, three known classes of sulfatases have been identified. Type I sulfatases rely on a post-translational modification to afford a catalytically active formylglycine residue for activity.[34] These sulfatases are known to cleave the $RO-SO_3^-$ bond, consuming one equivalent of water through a sulfated hemiacetal intermediate. Type III sulfatases utilize a Zn^{2+} cofactor to activate a water molecule for nucleophilic attack and cleave the same bond as type I sulfatases.[35] Curiously, type II alkyl sulfatases, which utilize a Fe^{2+} cofactor, are the only known enzyme in prokaryotes capable of cleaving the $R-OSO_3^-$ bond.[23] Many pathogenic bacteria are thought to utilize sulfatases in scavenging inorganic sulfates from the environment, and activity of sulfatases has been linked to several human diseases.[36]

Bertozzi and co-workers were the first to determine the structure and function of Rv3406 and found Rv3406 was essential for *Mtb* growth in sulfur-free media containing 2-ethylhexylsulfate (2-EHS) as the sole sulfur source.[23] Furthermore, the structure of Rv3406 shares a 54% sequence identity and 66% sequence similarity with *Pseudomonas putida* AtsK.[23] The putative active sites of both enzymes are nearly identical and share a nonheme, α-ketoglutarate-dependent Fe(II) dioxygenases binding motif. Rv3406 possesses a typical H-X-D/E-X_n-H iron-binding triad where X is any amino acid, and an additional arginine residue is involved in α-ketoglutarate binding.[37] A proposed mechanism of Rv3406-mediated cleavage of 2-EHS and **1** is shown in Figure 3.

The oxidation mechanism is dependent on the proximity of Fe(II) ion to the corresponding oxidized carbon. Molecular dynamics simulations of **1**, **6**, and **7** in a model-built structure of Rv3406 suggest this could be due to the failure of the enzyme to turnover the 5′-C-methyl derivatives. On the basis of a comparative analysis of MD simulations of all three ligands, it is

DOI: 10.1021/acsinfecdis.8b00038
ACS Infect. Dis. XXXX, XXX, XXX−XXX

evident that steric interactions of the added methyl group in **7**, with the coordinating residues of the Fe(II) ion (including the conserved residue, histidine 97), forces the 5′ carbon to be positioned further away from the reaction center (Figure 4).

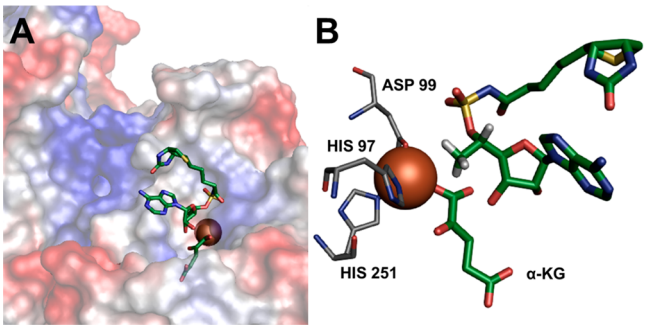

Figure 4. Simulated structure of 5′*S*-*C*-methyl Bio-AMS analog (**7**) in Rv3406. (A) Protein surface of Rv3406 with ligand, Fe(II) ion, and α-KG. Ligand **7** is solvent exposed and positioned unfavorably for oxidation of the 5′ carbon to occur. (B) Close up view of active site. The methyl sterically interferes with His97 and the Fe(II) ion.

This results in an unfavorable distance for hydrogen atom abstraction (Figure 3, step 4). In the case of the 5′*R*-*C*-methyl stereoisomer **6**, the results are not as clear. Average distances from the Fe(II) ion and the 5′ carbon were comparable for **1** and **6**, suggesting the 5′ carbon is accessible to oxidation. However, the simulations show the *R*-configured methyl of **6** crowds the active site, which may block entry of the O_2, ending the catalytic cycle. It is intuitive that further additions in the 5′ carbon region of **6** or **7** would only exacerbate this issue.

Interestingly, Cole and co-workers have reported overexpression of Rv3406 conferred resistance to an unrelated carboxyquinoxalines series of DprE1 inhibitors in *Mtb*.[38] Mutants were recovered at frequency of 1 in 10^{-6} that is approximately 10-fold greater than observed with **1**.[12] Whole-genome sequencing mapped resistant mutants to different nonsynonymous single nucleotide polymorphisms (SNP) or a single base deletion in the *rv3405c* gene, which led to a 30- to 47-fold increase in transcription levels of *rv3406*.[38] The mechanism of inactivation of the carboxyquinoxalines by Rv3406 occurs through decarboxylation leading to a biologically inactive keto derivative. The carboxyquinoxalines thus mimic the α-ketoglutarate substrate, whereas **1** mimics the alkyl sulfate. The carboxyquinoxalines were inactivated at rates similar to **1** with rates ranging from 0.02 to 1.07 min^{-1} versus 0.015 min^{-1} for **1**. The observation that overexpression of Rv3406 leads to oxidative destruction of two unrelated antitubercular agents is intriguing and further highlights the importance of TetR family transcriptional regulators (TFTR) in antibiotic resistance in mycobacteria.[39−41]

Although a variety of resistance mechanisms have been discovered for antitubercular agents, only a few examples of transcriptional dysregulation have been described leading to antibiotic inactivation. One recent example is Nathan and co-workers' discovery of a novel resistance mechanism involving *N*-methylation by the SAM-dependent methyltransferase Rv0560c.[42] Mutation to the transcriptional repressor *rv2887*, a member of the MarR family of DNA binding proteins, led to a more than 400-fold induction of *rv0560c*. Overexpression of Rv0560c completely ablated the biochemical and whole-cell activity of a pyrido-benzimiazole DprE1 inhibitor. Rv0560c and Rv3406 are both nonessential proteins, which are co-opted by *Mtb* to inactivate small molecules and illustrate the impressive ability of *Mtb* to spontaneously develop antibiotic resistance.

■ CONCLUSION

We successfully synthesized three analogues of **1** that maintained potent biochemical inhibition of *Mt*BPL and were not substrates for Rv3406 using an *in vitro* biochemical assay. 5′*R* Methyl-Bio-AMS **6** emerged as the most potent compound with an MIC of 1.56 μM against both WT *Mtb* and Rv3406-OE. We were unable to isolate resistant mutants to **6** at neither four nor ten times the agar MIC providing a frequency of resistance (FOR) of less than 1.44×10^{-10} compared to $(0.1-4) \times 10^{-6}$ for **1**. These data along with the biochemical and whole-cell activity, demonstrate modification of the nucleoside at the 5′-position overcame Rv3406-mediated resistance. Moreover, the low FOR of **6** indicates single step mutations in *Mtb* are unlikely to confer resistance to **6**. Overall, we believe this work nicely illustrates how a detailed molecular understanding of antibiotic inactivation can be used to guide the design of new analogues to overcome spontaneous resistance.

■ METHODS

***M. tuberculosis* MIC Assays and *Mt*BPL/Rv3406 Overexpression Strain Cloning.** MICs were experimentally determined as previously described using *M. tuberculosis* H37Rv grown in GAST medium [0.3 g/L Difco Bacto Casitone, 4.0 g/L K_2HPO_4, 2.0 g/L citric acid, 1.0 g/L L-alanine, 1.2 g/L $MgCl_2 \cdot 6\ H_2O$, 0.6 g/L K_2SO_4, 2.0 g/L NH_4Cl, 18 mM NaOH, 1% (v/v) glycerol, and 0.005% (v/v) Tween-80 or 0.05% Tyloxapol] with an initial inoculum of 10^5 CFU/mL in a 96- or 384-well plate.[20] The plates were incubated at 37 °C under 5% CO_2, and OD_{580} was measured after 14 or 18 days of incubation to monitor growth. MIC_{90} was defined as the concentration of the compound at which roughly 90% growth inhibition was observed compared to the no drug control. To study the resistance of these analogues toward degradation by Rv3406, the MICs were determined using the previously reported *Mtb* Rv3406 overexpression strain employing the assay conditions described above.[12] To confirm the engagement of **1** and **6** by *Mt*BPL, MICs were determined with the *Mt*BPL overexpression strain described previously using the same assay as mentioned above.[20]

***Mt*BPL and Rv3406 Expression and Purification.** *Mt*BPL and Rv3406 were cloned, overexpressed, and purified as previously described.[20,23]

Frequency of Resistance (FOR). The FOR for **6** was performed as previously described for **1**.[12] Briefly, the MIC of **6** on agar plates was determined by spotting approximately 10^6 bacteria onto 7H10 agar plates supplemented with OADC and varying drug concentrations. The lowest drug concentration where no growth was observed upon visual inspection after incubation at 37 °C for 3 weeks was used as the agar MIC. To isolate resistant mutants, approximately 7×10^9 bacteria were plated onto 7H10 agar plates supplemented with OADC and containing **6** at a concentration of 4× or 10× the agar MIC. After incubation at 37 °C for 3 weeks, colonies were counted. Plates without colonies were incubated for a further 6 weeks, and a final count was done at the end of 9 weeks of incubation. The initial number of bacteria was determined by plating dilutions of the original culture. FOR was calculated as the

DOI: 10.1021/acsinfecdis.8b00038
ACS Infect. Dis. XXXX, XXX, XXX−XXX

number of CFUs divided by the total number of bacteria plated for each concentration of **6**.

Isothermal Titration Calorimetry (ITC). All ITC experiments were conducted on an automated microcalorimeter (Malvern Instruments). The experiments were performed at 25 °C in ITC buffer (10 mM Tris, pH 7.5, 200 mM KCl, 2.5 mM $MgCl_2$). *Mt*BPL was exchanged (2 × 10 mL) into ITC buffer using an Amicon Ultra concentrator, and the final filtrate was used to prepare a solution of the analogues from a 10 mM stock in DMSO. Protein concentrations were 10 μM *Mt*BPL (determined by active site titration with **1**), 100 μM analogue, and 100 μM biotin (determined by weighing sample on an ultramicrobalance [Mettler Toledo] accurate to 0.001 mg). In the direct titration experiments, the analogue was injected into a solution of the enzyme. In the competitive titration experiments, the analogue was injected into a solution of the enzyme and biotin. Titrations were carried out with a stirring speed of 750 rpm and 200 s interval between 4 μL injections. The first injection for each sample was excluded from data fitting. Titrations were run past the point of enzyme saturation to correct for heats of dilution. The experimental data were fitted to a theoretical titration curve using the Origin software package (version 7.0) provided with the instrument to afford values of K_A^{app} (the apparent binding constant of the ligands in the presence of biotin in M^{-1}), n (stoichiometry of binding), and ΔH (the binding enthalpy change in kcal/mol). The K_A values for each ligand was obtained from the K_A^{app} value using eq 1:

$$K_A = K_A^{app}(1 + K_A^B[B]) \quad (1)$$

where $[B]$ is the concentration of biotin, and K_A^B is the association constant for biotin experimentally determined to be 7.29×10^5. The thermodynamic parameters (ΔG and ΔS) were calculated from K determined from the displacement titration and ΔH from the direct binding titration using eq 2.

$$\Delta G = -RT\ln(K) = \Delta H - T\Delta S \quad (2)$$

where ΔG, ΔH, and ΔS are the changes in free energy, enthalpy, and entropy of binding, respectively; R = 1.98 cal mol^{-1} K^{-1}; T is the absolute temperature (298 K). The affinity of the ligands for the protein is given as the dissociation constant ($K_D = 1/K_A$). ITC experiments were run in triplicate and analyzed independently, and the thermodynamic values were averaged.

Incubations of 6 and 7 with Rv3406. Assay conditions were adapted and modified from previous conditions with **1**.[12] All reactions were performed in 100 μL at 37 °C. Complete assay contained 40 mM Tris acetate buffer, pH 7.5, 50 mM NaCl, 0.2% triton, 100 μM iron(II) chloride, 1 mM α-ketoglutarate (α-KG), 2 mM ascorbate, and substrate (either **6** or **7**). The concentrations of substrate were tested at 4, 2, 1, 0.5, 0.25, 0.125, 0.0625, and 0 mM. Reactions were started by the addition of 6.6 μL of Rv3406 (stock 1.517 mg/mL), making the concentration of Rv3406 exactly 3 μM. Negative control reactions with respect to protein lacked Rv3406 while positive controls employed Bio-AMS as substrate. Both test and control reactions were run in duplicate. Reactions incubated in a 37 °C water bath; aliquots (30 μL) were withdrawn at 0 and 60 min and immediately quenched with 300 μL of 4:1 MeOH/acetone + 150 nM biotin (as an internal standard) to precipitate the protein. Samples were then centrifuged *in vacuo* for 30 min at 5000 rcf. The residue leftover after centrifugation was dissolved in 1 mL of 95:5 water/MeCN + 0.1% formic acid, and 100 μL aliquots were used for LC-MS/MS analysis.

Incubations of 8 and 9 with Rv3406. All reactions were performed in 100 μL at 37 °C. Complete assay contained 40 mM Tris acetate buffer, pH 7.5, 50 mM NaCl, 0.2% triton, 100 μM iron(II) chloride, 1 mM α-ketoglutarate (α-KG), 2 mM ascorbate, and 250 μM substrate (either **8** or **9**). Reactions were started by the addition of 6.6 μL of Rv3406 (stock 1.517 mg/mL), making the concentration of Rv3406 exactly 3 μM. Reaction time points were run at 0 and 60 min and immediately quenched with 300 μL of 10% aqueous TCA (trichloroacetic acid) + 200 nM biotin (as an internal standard) to precipitate the protein. All reactions were run in triplicate. Samples were then centrifuged for 10 min at 15 000 rcf. The supernatant was diluted 1:20 in 95:5 H_2O/MeCN + 0.5% formic acid, and 100 μL aliquots were used for LC-MS/MS analysis.

LC-MS/MS Analysis. Samples were analyzed by LC-MS/MS (Shimadzu UFLC XR-AB SCIEX QTRAP 5500). Reverse-phase LC was performed on a Kinetix C18 column (50 mm × 2.1 mm, 2.6 μm particle size; Phenomenex, Torrance, CA). Mobile phase A was 0.1% aqueous formic acid while mobile phase B was 0.1% formic acid in acetonitrile. Initial conditions were 5% B from 0 to 0.5 min, after which the %B was increased to 95% from 0.5 to 3 min. The column was washed in 95% B for 2 min, returned to 5% over 0.2 min, and allowed to re-equilibrate for 2.8 min in 5% B to provide a total run time of 8 min. The flow rate was 0.5 mL/min, and the column oven was maintained at 40 °C. The injection volume was 10 μL. All analytes from analogues **6** and **7** were analyzed by MS in negative ionization mode by multiple reaction monitoring (MRM), while all analytes from analogues **8** and **9** were analyzed by MS in positive ionization mode by MRM. The mass spectrometry settings were optimized by direct infusion of authentic standards for **8**, **9**, **S3**, and biotin. The collision energy ranged from +20 to +36 for positive mode and −40 for negative mode. The declustering potential was +35 for positive mode and −35 for negative mode. The following transitions were utilized: m/z 571.1 $[M + H]^+ \rightarrow m/z$ 227.1 $[\text{biotin} - H_2O + H]^+$, m/z 571.1 $[M + H]^+ \rightarrow m/z$ 244.1, m/z 571.1 $[M + H]^+ \rightarrow m/z$ 136.1 $[\text{adenine} + H]^+$ for **8**; m/z 571.1 $[M + H]^+ \rightarrow m/z$ 227.1 $[\text{biotin} - H_2O + H]^+$, m/z 571.1 $[M + H]^+ \rightarrow m/z$ 136.1 $[\text{adenine} + H]^+$ for **9**; m/z 322.1 $[M - H]^- \rightarrow m/z$ 196.1 for **S3**; m/z 587.1 $[M + H]^+ \rightarrow m/z$ 227.1 $[\text{biotin} - H_2O + H]^+$, m/z 587.1 $[M + H]^+ \rightarrow m/z$ 244.1, m/z 587.1 $[M + H]^+ \rightarrow m/z$ 136.1 $[\text{adenine} + H]^+$ for **S5**; m/z 585.1 $[M + H]^+ \rightarrow m/z$ 227.1 $[\text{biotin} - H_2O + H]^+$ for **S6**; m/z 307.1 $[M + H]^+$ for **S7**; m/z 295.1 $[M + H]^+$ for **S8**; m/z 603.1 $[M + H]^+ \rightarrow m/z$ 227.1 $[\text{biotin} - H_2O + H]^+$ for **S10**; m/z 245.1 $[M + H]^+ \rightarrow m/z$ 227.1 $[M - H_2O + H]^+$, m/z 243.1 $[M - H]^- \rightarrow m/z$ 200.0 for biotin. Analyte and internal standard peak areas were calculated (MultiQuant, version 2.0.2, AB SCIEX). Analyte peak areas were normalized to internal standard peak areas, and the analyte concentrations were determined with an appropriate standard curve.

General Materials and Methods. Chemicals and solvents were purchased from Acros Organics, Alfa Aesar, Sigma-Aldrich, and TCI America and were used as received. The nucleoside 2′,3′-*O*-isopropylideneadenosine **10** was obtained from Carbosynth (Berkshire, UK). N^6-Benzoyl-2′,3′-*O*-isopropylideneadenosine, **15**,[43] *N*-Boc-diphenylphosphorylmethanesulfonamide,[44] sulfamoyl chloride,[45] D-(+)-biotin *N*-hydroxysuccinimide ester,[46] and 5′-[*N*-(D-biotinoyl)sulfamoyl]amino-5′-deoxyadenosine triethylammonium salt (Bio-AMS), **1**,[20]

DOI: 10.1021/acsinfecdis.8b00038
ACS Infect. Dis. XXXX, XXX, XXX−XXX

were prepared as described. An anhydrous solvent dispensing system using two packed columns of neutral alumina was used for drying THF and CH_2Cl_2, while two packed columns of molecular sieves were used to dry DMF, and the solvents were dispensed under argon (Ar). Anhydrous grade MeOH, MeCN, pyridine, and DMA were purchased from Aldrich. EtOAc and hexanes were purchased from Fisher Scientific. All reactions were performed under an inert atmosphere of dry argon (Ar) in oven-dried (180 °C) glassware. TLC analyses were performed on TLC silica gel plates 60F254 from EMD Chemical Inc. and were visualized with UV light. Optical rotations values were obtained on a polarimeter using a 1 dm cell. Purification by flash chromatography was performed using a medium-pressure flash chromatography system equipped with flash column silica cartridges with the indicated solvent system. Preparative reversed-phase HPLC purification was performed on a Phenomenex Gemini 10 μm C18 250 × 20 mm column operating at 21.0 mL/min with detection at 254 nm with the indicated solvent system. Analytical reversed-phase HPLC was performed on a Phenomenex Gemini 5 μm C18 250 × 4.6 mm column operating at 1 mL/min with detection at 254 nm employing a linear gradient from 5% to 50% MeCN in 50 mM aqueous triethylammonium bicarbonate (TEAB) at pH 7.5 for 30 min (Method A) or operating at 0.8 mL/min with detection at 260 nm employing a linear gradient from 30% to 70% MeOH with 0.1% TFA in H_2O with 0.1% TFA for 29 min (Method B). ^{1}H and ^{13}C spectra were recorded on 400 or 500 MHz NMR spectrometers. Proton chemical shifts are reported in ppm from an internal standard of residual chloroform (7.27), methanol (3.31), or dimethyl sulfoxide (2.50); carbon chemical shifts are reported in ppm from an internal standard of residual chloroform (77.0), methanol (49.1), or dimethyl sulfoxide (39.5). Proton chemical data are reported as follows: chemical shift, multiplicity (s = singlet, d = doublet, dt = doublet of triplets, t = triplet, q = quartet, pentet = pent, m = multiplet, ap = apparent, br = broad, ovlp = overlapping), coupling constant(s), and integration. High-resolution mass spectra were obtained on an LTQ Orbitrap Velos instrument (Thermo Scientific, Waltham, MA). All compounds were determined to be >95% by analytical reverse-phase HPLC (purities for each final compound are given in the experimental section below).

***N*^{6}-Benzoyl-5′-deoxy-2′,3′-*O*-isoproylideneadenosine-5′-methylcarbonyl (16).** To a solution of **S18** (4.0 g, 8.54 mmol, 1.0 equiv) in THF (55 mL) cooled to −20 °C (10% EtOH/ethylene glycol, dry ice bath) was added a solution of methylmagnesium bromide in THF (3 M, 3.41 mL, 10.2 mmol, 1.2 equiv). The reaction was stirred for 30 min, followed by addition of another equivalent of methylmagnesium bromide in THF (3 M, 3.13 mL, 9.39 mmol, 1.1 equiv). The reaction was stirred at −20 °C for 4 h and then quenched carefully with saturated aqueous NH_4Cl (30 mL; *caution: methane gas evolution*). Organic products were diluted with EtOAc (50 mL). Combined organic layers were washed successively with H_2O (50 mL), and saturated aqueous NaCl (50 mL), then dried ($MgSO_4$), and concentrated *in vacuo* to afford an off-white foam. Purification by flash chromatography (0−5% MeOH−CH_2Cl_2 stepwise gradient) afforded the title compound (3.18 g, 88%) as a white foam: R_f = 0.37 (5% MeOH/CH_2Cl_2); R_f = 0.35 (EtOAc); $[\alpha]_D^{23}$ − 38.0° (*c* 1.00, MeOH); ^{1}H NMR (400 MHz, $CDCl_3$) δ 1.43 (s, 3H), 1.64 (s, 3H), 1.96 (s, 3H), 4.69 (d, *J* = 2.7 Hz, 1H), 5.41 (d, *J* = 5.9 Hz, 1H), 5.59 (dd, *J* = 6.3, 2.3 Hz, 1H), 6.27 (s, 1H), 7.46−7.58 (m, 2H), 7.62 (d, *J* = 7.4 Hz, 1H), 8.04 (d, *J* = 7.4 Hz, 2H), 8.18 (s, 1 H), 8.71 (s, 1 H); ^{13}C NMR (100 MHz, $CDCl_3$) δ 25.2, 26.0, 26.8, 82.7, 84.2, 91.6, 93.2, 114.5, 123.0, 127.9, 128.9, 133.0, 133.3, 142.5, 149.7, 151.0, 152.3, 164.5, 204.9; HRMS (ESI+) calcd for $C_{21}H_{21}N_5O_5Na$ [M + Na]$^+$, 446.1435; found, 446.1472.

***N*^{6}-Benzoyl-2′,3′-*O*-isopropylidene-(5′*R*)-5′-*C*-methyladenosine (17).** A solution of sodium formate (6.8 g, 99.2 mmol) in H_2O (40 mL) was added to a 100 mL round-bottom flask charged with **16** (1.00 g, 2.36 mmol, 1.0 equiv) and η^6-(*p*-cymene)-(*R*,*R*)-*N*-toluenesulfonyl-1,2-diphenylethylenediamine(1−)ruthenium(II) chloride (16 mg, 0.0236 mmol, 1 mol %). EtOAc (10 mL) was then added, and reaction mixture was stirred for 2 d at 23 °C during which some solid precipitated from the solution. After 2 d, reaction was diluted with additional CH_2Cl_2 (30 mL), and the aqueous layer was separated. The organic layer was concentrated *in vacuo* to afford a dark amber residue which was redissolved in EtOAc (20 mL) and transferred to a beaker (100 mL). H_2O (10 mL) was then added, and the layers were covered and stirred at 23 °C overnight. A white solid precipitated and was collected by filtration, washed with MBTE (2 × 10 mL), and dried *in vacuo* to afford the title compound (0.55 g, 55%) as a white solid: R_f = 0.33 (5% MeOH/CH_2Cl_2); R_f = 0.12 (EtOAc); HPLC purity: 99.0%, t_R = 17.45 min, k' = 3.30 (method B); $[\alpha]_D^{23}$ − 64.1° (*c* 1.00, MeOH); ^{1}H NMR (400 MHz, DMSO-d_6) δ 1.04 (d, *J* = 6.3 Hz, 3H), 1.35 (s, 3H), 1.56 (s, 4H), 3.67−3.82 (m, 1H), 3.98 (dd, *J* = 5.5, 2.7 Hz, 1H), 5.10 (dd, *J* = 6.3, 2.3 Hz, 1H), 5.18 (d, *J* = 4.3 Hz, 1H), 5.41 (dd, *J* = 6.3, 3.1 Hz, 1H), 6.26 (d, *J* = 2.7 Hz, 1H), 7.55 (t, *J* = 7.4 Hz, 2H), 7.65 (t, *J* = 7.4 Hz, 1H), 7.98−8.14 (m, 2H), 8.68 (s, 1H), 8.77 (s, 1H), 11.25 (br s, 2H); ^{13}C NMR (100 MHz, DMSO-d_6) δ 19.7, 25.2, 27.1, 66.1, 80.4, 83.2, 89.4, 90.1, 113.1, 125.6, 128.45, 128.48, 132.4, 133.3, 143.2, 150.5, 151.8, 165.7; HRMS (ESI+) calcd for $C_{21}H_{23}N_5O_5Na$ [M + Na]$^+$, 448.1591; found, 448.1585.

***N*^{6}-Benzoyl-2′,3′-*O*-isopropylidene-(5′*R*)-5′-*C*-methyl-5′-*O*-sulfamoyladenosine (19).** To a solution of **17** (0.15 g, 0.35 mmol, 1.0 equiv) in dimethoxyethane (2 mL) cooled to 0 °C was added sodium hydride (21 mg, 0.53 mmol, 1.5 equiv, 60% in mineral oil) in one portion. The reaction was stirred at 0 °C until H_2 evolution ceased and the mixture became a thick slurry (40 min). To the reaction was then added dropwise a solution of freshly prepared sulfamoyl chloride (0.12 g, 1.1 mmol, 3.0 equiv) in MeCN (2 mL). After 16 h, the reaction was quenched with triethylamine/MeOH (1:1, 1 mL) and concentrated *in vacuo* to afford an off-white gel. The product was extracted with EtOAc (30 mL), successively washed with H_2O (30 mL), and saturated aqueous NaCl (30 mL), then dried ($MgSO_4$), and concentrated to afford an off-white foam. Purification by flash chromatography (50−100% EtOAc/Hexanes, linear gradient) afforded the title compound (0.11 g, 62%) as a white solid: R_f = 0.49 (EtOAc); ^{1}H NMR (500 MHz, MeOH-d_4) δ 1.37 (d, *J* = 6.4 Hz, 3H), 1.41 (s, 3H), 1.63 (s, 3H), 4.20 (dd, *J* = 6.0, 3.5 Hz, 1H), 4.83−4.86 (m, ovlp with HDO, 1H), 5.33 (dd, *J* = 6.4, 3.4 Hz, 1H), 5.47 (dd, *J* = 6.4, 2.7 Hz, 1H), 6.34 (d, *J* = 2.7 Hz, 1H), 7.52−7.62 (m, 2H), 7.63−7.70 (m, 1H), 7.98−8.20 (m, 2H), 8.57 (s, 1H), 8.76 (s, 1H); ^{13}C NMR (125 MHz, MeOH-d_4) δ 17.8, 25.7, 27.7, 78.0, 82.3, 85.3, 89.8, 91.6, 116.0, 125.5, 129.6, 129.9, 134.1, 135.1, 145.0, 151.5, 153.1, 153.7; HRMS (ESI+) calcd for $C_{21}H_{25}N_6O_7SNa$ [M + Na]$^+$, 528.1398; found, 528.1411.

(5′*R*)-5′-*O*-[*N*-(D-Biotinoyl)sulfamoyl]-5′-*C*-methyladenosine Triethylammonium Salt (6). To a solution of **19** (100 mg, 0.198 mmol, 1.0 equiv) and Cs_2CO_3 (161 mg, 0.500 mmol, 2.5 equiv) in DMF (2 mL) at 0 °C was added D-

DOI: 10.1021/acsinfecdis.8b00038
ACS Infect. Dis. XXXX, XXX, XXX−XXX

(+)-biotin *N*-hydroxysuccinimide ester (102 mg, 0.297 mmol, 1.5 equiv). The reaction mixture was stirred for 16 h at 23 °C during which time all starting material was consumed as monitored by TLC. DMF was removed *in vacuo*, redissolved in MeOH−CH_2Cl_2 (1:9, 5 mL), filtered through Celite, and concentrated *in vacuo* to afford crude biotinylated nucleoside. The crude product was used in the next deprotection reactions directly without further purification.

The crude material was dissolved in pyridine (1 mL), and saturated aqueous ammonia (1 mL) was added. The reaction was stirred at 23 °C in a sealed vessel. After 2 d, the reaction was concentrated under high vacuum (P = 0.05 Torr). The crude debenzoylated material was redissolved in 80% aqueous trifluoroacetic acid (5 mL) and stirred for 2 h at 23 °C. The crude material was then concentrated *in vacuo* and redissolved in 1:1 MeCN/50 mM TEAB (10−20 mg/mL) and filtered to remove insoluble solids. The resulting solution was purified by preparative reverse phase HPLC with a Phenomenx Gemini C18 (250 × 20 mm) column at a flow rate of 21.0 mL/min employing a linear gradient of 5−50% acetonitrile (solvent B) in 50 mM aqueous triethylammonium bicarbonate (TEAB) at pH 7.0 (solvent A) for 30 min. The appropriate fractions were pooled and lyophilized to afford the title compound (38 mg, 33% over 3 steps) as the triethylammonium salt (2.4 equiv of Et_3N) as a white solid: HPLC purity: 99.0%, t_R = 13.30 min, k' = 2.2 (method A); ^{1}H NMR (500 MHz, MeOH-d_4) δ 1.10 (t, J = 7.3 Hz, 28H, excess Et_3N), 1.20−1.24 (m, 1H), 1.42 (d, J = 6.4 Hz, 3H), 1.42−1.45 (m ovlp, 1H), 1.49−1.66 (m, 3H), 1.66−1.79 (m, 1H), 2.19 (td, J = 7.5, 1.8 Hz, 2H), 2.69 (q, J = 7.2 Hz, 19H, excess Et_3N), 2.89 (dd, J = 12.7, 5.0 Hz, 1 H), 3.16 (ddd, J = 8.3, 6.2, 4.7 Hz, 1H), 3.98 (dd, J = 4.7, 2.6 Hz, 1H), 4.29 (dd, J = 7.9, 4.6 Hz, 1H), 4.46 (dd, J = 7.6, 4.3 Hz, 1H), 4.49 (dd, J = 5.3, 2.6 Hz, 1H), 4.74 (dd, J = 6.9, 5.3 Hz, 1H), 6.03 (d, J = 7.0 Hz, 1H), 8.21 (s, 1H), 8.59 (s, 1H); ^{13}C NMR (125 MHz, MeOH-d_4) δ 10.9, 18.0, 27.3, 29.6, 30.1, 40.3, 41.2, 47.3, 57.1, 61.7, 63.4, 71.6, 75.6, 77.4, 88.5, 89.0, 120.4, 142.0, 151.2, 154.0, 157.4, 183.1; HRMS (ESI−) calcd for $C_{21}H_{29}N_8O_8S_2^-$ [M − Et_3NH]$^-$, 585.1555; found, 585.1516.

***N*^{6}-Benzoyl-2′,3′-*O*-isopropylidene-(5′*S*)-5′-*C*-methyladenosine (18).** A solution of sodium formate (6.8 g, 99.2 mmol) in H_2O (40 mL) was added to a 100 mL round-bottom flask charged with **16** (1.00 g, 2.36 mmol, 1.0 equiv) and η^6-(*p*-cymene)-(*S*,*S*)-*N*-toluenesulfonyl-1,2-diphenylethylenediamine-(1−)ruthenium(II) chloride (16 mg, 0.0236 mmol, 1 mol %). EtOAc (10 mL) was then added, and the reaction mixture was stirred at 23 °C during which some solid precipitated from the solution. After 22 h, the reaction was diluted with additional EtOAc (20 mL), and the aqueous layer was separated. The organic layer was concentrated *in vacuo* to afford a dark amber solid which was resuspended in EtOAc (12 mL) and heptane (8 mL). The suspension was heated to 80 °C for 15 min and slowly cooled to 23 °C with stirring during which a solid precipitated. The solid was collected by filtration and dried *in vacuo* to afford the title compound (0.61 g, 61%) as an off-white solid: mp = 166−167 °C; R_f = 0.33 (5% MeOH/CH_2Cl_2); R_f = 0.12 (EtOAc); HPLC purity: 99.0%, t_R = 17.18 min, k' = 3.23 (method B); $[\alpha]_D^{23}$ − 44.9° (c 1.00, MeOH); ^{1}H NMR (400 MHz, DMSO-d_6) δ 1.11 (d, J = 6.3 Hz, 3H), 1.34 (s, 3H), 1.57 (s, 3H), 3.71−3.89 (m, 1H), 4.07 (dd, J = 4.3, 3.1 Hz, 1H), 4.97 (dd, J = 6.1, 2.9 Hz, 1H), 5.14 (d, J = 5.1 Hz, 1H), 5.34 (dd, J = 6.3, 3.1 Hz, 1H), 6.28 (d, J = 3.1 Hz, 2H), 7.56 (t, J = 7.6 Hz, 2H), 7.65 (t, J = 7.2 Hz, 1H), 7.99−8.11 (m, 2H), 8.75 (s, 1H), 8.77 (s, 1H), 11.21 (s, 1H); ^{13}C NMR (100 MHz, DMSO-d_6) δ 19.2, 25.3, 27.2, 66.3, 81.4, 83.5, 89.3, 89.6, 113.1, 125.6, 128.5, 132.4, 133.3, 143.1, 150.4, 151.7, 151.9, 165.6; HRMS (ESI+) calcd for $C_{21}H_{23}N_5O_5Na$ [M + Na]$^+$, 448.1591; found, 448.1614.

***N*^{6}-Benzoyl-2′,3′-*O*-isopropylidene-(5′*S*)-5′-*C*-methyl-5′-*O*-sulfamoyladenosine (20).** To a solution of **18** (0.20 g, 0.47 mmol, 1.0 equiv) in dimethoxyethane (2 mL) cooled to 0 °C was added sodium hydride (28 mg, 0.71 mmol, 1.5 equiv, 60% in mineral oil) in one portion. The reaction was stirred at 0 °C until H_2 evolution ceased and the mixture became a thick slurry (40 min). To the reaction was then added dropwise a solution of freshly prepared sulfamoyl chloride (0.16 g, 1.4 mmol, 3 equiv) in MeCN (2 mL). After 3 h, the reaction was quenched with triethylamine/MeOH (1:1, 1 mL) and concentrated *in vacuo* to afford an off-white gel. The product was extracted with EtOAc (30 mL), washed with H_2O (30 mL), saturated aqueous NaCl (30 mL), dried ($MgSO_4$), and concentrated to afford an off-white foam. Purification by flash chromatography (50−100% EtOAc/Hexanes, linear gradient) afforded the title compound (0.19 g, 80%) as a white solid: R_f = 0.49 (EtOAc); ^{1}H NMR (500 MHz, MeOH-d_4) δ 1.41 (s, 3H), 1.45 (d, J = 6.4 Hz, 3H), 1.63 (s, 3H), 4.36 (dd, J = 3.7, 3.1 Hz, 1H), 4.79 (qd, J = 6.5, 4.0 Hz, 1H), 5.16 (dd, J = 6.1, 2.7 Hz, 1H), 5.42 (dd, J = 6.1, 2.7 Hz, 1H), 6.41 (d, J = 2.7 Hz, 1H), 7.40−7.62 (m, 2H), 7.62−7.73 (m, 1H), 8.01−8.20 (m, 2H), 8.59 (s, 1H), 8.74 (s, 1H); ^{13}C NMR (125 MHz, MeOH-d_4) δ 17.4, 25.7, 27.7, 78.9, 83.4, 85.6, 89.9, 91.8, 115.6, 125.1, 129.6, 129.9, 134.1, 135.1, 144.4, 151.3, 153.51, 153.53, 168.4; HRMS (ESI+) calcd for $C_{21}H_{25}N_6O_7SNa$ [M + Na]$^+$, 528.1398; found, 528.1411.

(5′*S*)-5′-*O*-[*N*-(D-Biotinoyl)sulfamoyl]-5′-*C*-methyladenosine Triethylammonium Salt (7). To a solution of **20** (190 mg, 0.377 mmol, 1.0 equiv) and Cs_2CO_3 (307 mg, 0.941 mmol, 2.5 equiv) in DMF (4 mL) at 0 °C was added D-(+)-biotin *N*-hydroxysuccinimide ester (193 mg, 0.565 mmol, 1.5 equiv). The reaction mixture was stirred for 16 h at 23 °C during which time all starting material was consumed as monitored by TLC. DMF was removed *in vacuo*, and the residue was redissolved in MeOH−CH_2Cl_2 (1:9, 10 mL), filtered through Celite, and concentrated *in vacuo* to afford crude biotinylated nucleoside. The crude product was used in the next deprotection reactions directly without further purification.

The crude material was dissolved in pyridine (1 mL), and saturated aqueous ammonia (1 mL) was added. The reaction stirred at 23 °C in a sealed vessel. After 2 d, the reaction was concentrated under high vacuum (P = 0.05 Torr). The crude debenzoylated material was redissolved in 80% aqueous trifluoroacetic acid (5 mL) and stirred for 2 h at 23 °C. The crude material was then concentrated *in vacuo* and redissolved in 1:1 MeCN/50 mM TEAB (10−20 mg/mL) and filtered to remove insoluble solids. The resulting solution was purified by preparative reverse phase HPLC with a Phenomenx Gemini C18 (250 × 20 mm) column at a flow rate of 21.0 mL/min employing a linear gradient of 5−50% acetonitrile (solvent B) in 50 mM aqueous triethylammonium bicarbonate (TEAB) at pH 7.0 (solvent A) for 30 min. The appropriate fractions were pooled and lyophilized to afford the title compound (56 mg, 22% over 3 steps) as the triethylammonium salt (1.5 equiv of Et_3N) as a white solid: HPLC purity: 99.2%, t_R = 12.86 min, k' = 2.5 (method A); ^{1}H NMR (500 MHz, MeOH-d_4) δ 1.15 (t, J = 7.3 Hz, 9H, excess Et_3N), 1.23−1.30 (m, 1H), 1.46 (d, J = 6.4 Hz, 3H), 1.56−1.79 (m, 4H), 2.24 (td, J = 7.4, 2.6 Hz, 2H),

DOI: 10.1021/acsinfecdis.8b00038
ACS Infect. Dis. XXXX, XXX, XXX−XXX

2.68 (d, J = 12.8 Hz, 1H), 2.79 (q, J = 7.3 Hz, 13H, excess Et_3N), 2.86−2.98 (m, 2H), 3.15−3.23 (m, 1H), 4.10 (dd, J = 2.7, 1.8 Hz, 1H), 4.30 (dd, J = 7.9, 4.6 Hz, 1H), 4.46 (dd, J = 7.9, 4.3 Hz, 1H), 4.50 (dd, J = 5.0, 2.9 Hz, 1H), 4.72−4.78 (m, 1H), 4.85 (dd, J = 6.6, 1.7 Hz, 1H), 6.14 (d, J = 6.1 Hz, 1H), 8.22 (s, 1H), 8.56 (s, 1H); ^{13}C NMR (125 MHz, MeOH-d_4) δ 9.1, 16.7, 25.8, 28.0, 28.4, 38.6, 39.7, 45.9, 47.8, 48.1, 55.5, 60.2, 61.8, 71.6, 75.0, 75.4, 87.1, 87.8, 139.5, 149.7, 152.5, 181.7; HRMS (ESI−) calcd for $C_{21}H_{29}N_8O_8S_2^-$ [M − Et_3NH]$^-$, 585.1555; found, 585.1599.

(*E*)-*N*-Biotinoyl-*C*-(5′-adenosylidene)-methanesulfonamide Triethylammonium Salt (9). To a solution of **22** (21 mg, 0.055 mmol, 1.0 equiv) and Cs_2CO_3 (54 mg, 0.165 mmol, 3 equiv) in DMF (3 mL) at 0 °C was added D-(+)-biotin *N*-hydroxysuccinimide ester (38 mg, 0.11 mmol, 2 equiv). The reaction mixture was stirred for 16 h at 23 °C during which time all starting material was consumed as monitored by TLC. DMF was removed *in vacuo*, and the residue was redissolved in MeOH−CH_2Cl_2 (1:9, 5 mL), filtered through Celite, and concentrated *in vacuo* to afford crude biotinylated nucleoside. The crude product was used in the next deprotection reactions directly without further purification.

The crude coupled product was dissolved in 80% aqueous trifluoroacetic acid (5 mL) and stirred for 2 h at 23 °C. The crude material was then concentrated *in vacuo* and redissolved in 1:1 MeCN/50 mM TEAB (10−20 mg/mL) and filtered to remove insoluble solids. The resulting solution was purified by preparative reverse phase HPLC with a Phenomenx Gemini C18 (250 × 20 mm) column at a flow rate of 21.0 mL/min employing a linear gradient of 5−50% acetonitrile (solvent B) in 50 mM aqueous triethylammonium bicarbonate (TEAB) at pH 7.0 (solvent A) for 30 min. The appropriate fractions were pooled and lyophilized to afford the title compound (19 mg, 52% over 3 steps) as the triethylammonium salt (1.1 equiv of Et_3N) as a white solid: ^{1}H NMR (500 MHz, DMSO-d_6) δ 0.89 (t, J = 7.1 Hz, 9H, Et_3N), 1.01−0.96 (m, 1H), 1.30−1.20 (m, 3H), 1.48−1.34 (m, 3H), 1.61−1.54 (m, 1H), 1.89 (t, J = 7.4 Hz, 2H), 2.39 (q, J = 7.1 Hz, 6H, Et_3N), 2.56−2.50 (m, 1H), 2.78 (ddd, J = 12.4, 7.2, 5.1 Hz, 1H), 3.04 (dq, J = 6.1, 4.0 Hz, 1H), 4.13−4.06 (m, 2H), 4.28−4.23 (m, 2H), 4.38 (ddd, J = 5.9, 4.6, 1.5 Hz, 1H), 4.56 (t, J = 5.2 Hz, 1H), 5.91 (d, J = 5.2 Hz, 1H), 6.31 (br s, 1H), 6.38 (dd, J = 15.4, 6.0 Hz, 1H), 6.46 (s, 1H), 6.68 (dd, J = 15.3, 1.4 Hz, 1H), 7.29 (s, 2H), 8.11 (s, 1H), 8.28 (s, 1H); ^{13}C NMR (125 MHz, DMSO-d_6) δ 11.7, 25.9, 28.1, 28.4, 39.8, 45.7, 55.5, 59.2, 61.0, 72.9, 73.7, 82.4, 87.3, 119.0, 132.8, 135.6, 139.5, 149.5, 152.7, 156.1, 162.8, 178.1; HRMS (ESI−) calcd for $C_{21}H_{29}N_8O_8S_2^-$ [M − Et_3NH]$^-$, 567.1450; found, 567.1454.

■ ASSOCIATED CONTENT

Supporting Information

The Supporting Information is available free of charge on the ACS Publications website at DOI: 10.1021/acsinfecdis.8b00038.

Growth inhibition concentration−response plots for determination of MIC values, all experimental ITC data, HPLC traces for final compounds, LC-MS/MS parameters and fragmentation data, proposed metabolic pathways by Rv3406 for **6**−**9**, synthetic procedures for **13**, **S9**, and **S18**, and ^{1}H and ^{13}NMR spectra of all described compounds (PDF)

■ AUTHOR INFORMATION

Corresponding Author

*Phone: 612-625-7956. Fax: 612-626-3114. E-mail: aldri015@umn.edu.

ORCID

David M. Ferguson: 0000-0001-6294-8057

Courtney C. Aldrich: 0000-0001-9261-594X

Author Contributions

The manuscript was written with contributions of all authors. All authors have given approval to the final version of the manuscript.

Notes

The authors declare no competing financial interest.

■ ACKNOWLEDGMENTS

This work was supported by a grant (AI091790 to D.S.) from the National Institutes of Health as well as the University of Minnesota Bighley Fellowship. Isothermal titration calorimetry was carried out using an ITC-200 microcalorimeter, funded by the NIH Shared Instrumentation Grant S10-OD017982. Mass spectrometry was carried out in the Center for Mass Spectrometry and Proteomics, University of Minnesota. We also gratefully acknowledge Bruce Witthuhn for his contributions and assistance using the LC-MS/MS instruments. We also thank Carolyn Bertozzi for providing the Rv3406 overexpression plasmid. Finally, we acknowledge the Minnesota Supercomputing Institute (MSI) at the University of Minnesota for providing resources that contributed to the research results reported within this paper (http://www.msi.umn.edu).

■ ABBREVIATIONS

ACCs, acyl CoA carboxylases; Bio-AMS, 5′-[*N*-(D-biotinoyl)-sulfamoyl]amino-5′-deoxyadenosine; Bio-NHS, D-(+)-biotin *N*-hydroxysuccinimide ester; TEMPO, (2,2,6,6-tetramethylpiperidin-1-yl)oxyl; Boc, *tert*-butyloxycarbonyl; (*R*,*R*)-TsDPEN, η^6-(*p*-cymene)-(*R*,*R*)-*N*-toluenesulfonyl-1,2-diphenylethylenediamine(1−)ruthenium(II) chloride; (*S*,*S*)-TsDPEN, η^6-(*p*-cymene)-(*S*,*S*)-*N*-toluenesulfonyl-1,2-diphenylethylenediamine(1−)ruthenium(II) chloride; HPLC, high performance liquid chromatography; LC-MS/MS, liquid chromatography tandem mass spectrometry; ITC, isothermal titration calorimetry; MIC, minimum inhibitory concentration; *Mtb*, *Mycobacterium tuberculosis*; *Mt*BPL, *Mycobacterium tuberculosis* biotin protein ligase; TB, tuberculosis; TFA, trifluoroacetic acid; MDR-TB, multidrug resistant tuberculosis; XDR-TB, extensively drug resistant tuberculosis

■ REFERENCES

(1) WHO. (2015) *Global tuberculosis report*, World Health Organization, Geneva, Switzerland.

(2) Gokhale, R. S., Saxena, P., Chopra, T., and Mohanty, D. (2007) Versatile polyketide enzymatic machinery for the biosynthesis of complex mycobacterial lipids. *Nat. Prod. Rep. 24*, 267−277.

(3) Onwueme, K. C., Vos, C. J., Zurita, J., Ferreras, J. A., and Quadri, L. E. (2005) The dimycocerosate ester polyketide virulence factors of mycobacteria. *Prog. Lipid Res. 44*, 259−302.

(4) Ishikawa, E., Ishikawa, T., Morita, Y. S., Toyonaga, K., Yamada, H., Takeuchi, O., Kinoshita, T., Akira, S., Yoshikai, Y., and Yamasaki, S. (2009) Direct recognition of the mycobacterial glycolipid, trehalose dimycolate, by C-type lectin Mincle. *J. Exp. Med. 206*, 2879−2888.

(5) Reed, M. B., Domenech, P., Manca, C., Su, H., Barczak, A. K., Kreiswirth, B. N., Kaplan, G., and Barry, C. E., 3rd (2004) A glycolipid

of hypervirulent tuberculosis strains that inhibits the innate immune response. *Nature 431*, 84−87.

(6) Cambier, C. J., Takaki, K. K., Larson, R. P., Hernandez, R. E., Tobin, D. M., Urdahl, K. B., Cosma, C. L., and Ramakrishnan, L. (2014) Mycobacteria manipulate macrophage recruitment through coordinated use of membrane lipids. *Nature 505*, 218−222.

(7) Goldberg, M. F., Saini, N. K., and Porcelli, S. A. (2014) Evasion of Innate and Adaptive Immunity by *Mycobacterium tuberculosis*. *Microbiol. Spectrum 2*, DOI: 10.1128/microbiolspec.MGM2-0005-2013.

(8) Ganapathy, U., Marrero, J., Calhoun, S., Eoh, H., de Carvalho, L. P. S., Rhee, K., and Ehrt, S. (2015) Two enzymes with redundant fructose bisphosphatase activity sustain gluconeogenesis and virulence in *Mycobacterium tuberculosis*. *Nat. Commun. 6*, 7912.

(9) Purushothaman, S., Gupta, G., Srivastava, R., Ramu, V. G., and Surolia, A. (2008) Ligand specificity of group I biotin protein ligase of *Mycobacterium tuberculosis*. *PLoS One 3*, e2320.

(10) Paparella, A. S., Soares da Costa, T. P., Yap, M. Y., Tieu, W., Wilce, M. C., Booker, G. W., Abell, A. D., and Polyak, S. W. (2014) Structure guided design of biotin protein ligase inhibitors for antibiotic discovery. *Curr. Top. Med. Chem. 14*, 4−20.

(11) Feng, J., Paparella, A. S., Booker, G. W., Polyak, S. W., and Abell, A. D. (2016) Biotin Protein Ligase Is a Target for New Antibacterials. *Antibiotics 5*, 26.

(12) Tiwari, D., Park, S. W., Essawy, M., Dawadi, S., Mason, A., Nandakumar, M., Zimmerman, M., Mina, M., Ho, H. P., Engelhart, C., Ioerger, T., Sacchettini, J., Rhee, K. Y., Ehrt, S., Aldrich, C. C., Dartois, V., and Schnappinger, D. (2018) Targeting protein biotinylation enhances tuberculosis chemotherapyy. *Sci. Transl. Med. 10*, eaal1803.

(13) Brown, P. H., Cronan, J. E., Grøtli, M., and Beckett, D. (2004) The biotin repressor: modulation of allostery by corepressor analogs. *J. Mol. Biol. 337*, 857−869.

(14) Sittiwong, W., Cordonier, E. L., Zempleni, J., and Dussault, P. H. (2014) *β*-Keto and *β*-hydroxyphosphonate analogs of biotin-5′-AMP are inhibitors of holocarboxylase synthetase. *Bioorg. Med. Chem. Lett. 24*, 5568−5571.

(15) Soares da Costa, T. P., Tieu, W., Yap, M. Y., Zvarec, O., Bell, J. M., Turnidge, J. D., Wallace, J. C., Booker, G. W., Wilce, M. C. J., Abell, A. D., and Polyak, S. W. (2012) Biotin analogues with antibacterial activity are potent inhibitors of biotin protein ligase. *ACS Med. Chem. Lett. 3*, 509−514.

(16) Tieu, W., Soares da Costa, T. P., Yap, M. Y., Keeling, K. L., Wilce, M. C. J., Wallace, J. C., Booker, G. W., Polyak, S. W., and Abell, A. D. (2013) Optimising *in situ* click chemistry: the screening and identification of biotin protein ligase inhibitors. *Chem. Sci. 4*, 3533−3537.

(17) Tieu, W., Jarrad, A. M., Paparella, A. S., Keeling, K. A., Soares da Costa, T. P., Wallace, J. C., Booker, G. W., Polyak, S. W., and Abell, A. D. (2014) Heterocyclic acyl-phosphate bioisostere-based inhibitors of *Staphylococcus aureus* biotin protein ligase. *Bioorg. Med. Chem. Lett. 24*, 4689−4693.

(18) Paparella, A. S., Lee, K. J., Hayes, A. J., Feng, J., Feng, Z., Cini, D., Deshmukh, S., Booker, G. W., Wilce, M. C. J., Polyak, S. W., and Abell, A. D. (2018) Halogenation of Biotin Protein Ligase Inhibitors Improves Whole Cell Activity against *Staphylococcus aureus*. *ACS Infect. Dis. 4*, 175.

(19) Feng, J., Paparella, A. S., Tieu, W., Heim, D., Clark, S., Hayes, A., Booker, G. W., Polyak, S. W., and Abell, A. D. (2016) New Series of BPL Inhibitors To Probe the Ribose-Binding Pocket of Staphylococcus aureus Biotin Protein Ligase. *ACS Med. Chem. Lett. 7*, 1068−1072.

(20) Duckworth, B. P., Geders, T. W., Tiwari, D., Boshoff, H. I., Sibbald, P. A., Barry, C. E., III, Schnappinger, D., Finzel, B. C., and Aldrich, C. C. (2011) Bisubstrate Adenylation Inhibitors of Biotin Protein Ligase from *Mycobacterium tuberculosis*. *Chem. Biol. 18*, 1432−1441.

(21) Shi, C., Tiwari, D., Wilson, D. J., Seiler, C. L., Schnappinger, D., and Aldrich, C. C. (2013) Bisubstrate Inhibitors of Biotin Protein Ligase in *Mycobacterium tuberculosis* Resistant to Cyclonucleoside Formation. *ACS Med. Chem. Lett. 4*, 1213−1217.

(22) Bockman, M. R., Kalinda, A. S., Petrelli, R., De la Mora-Rey, T., Tiwari, D., Liu, F., Dawadi, S., Nandakumar, M., Rhee, K. Y., Schnappinger, D., Finzel, B. C., and Aldrich, C. C. (2015) Targeting *Mycobacterium tuberculosis* Biotin Protein Ligase (*Mt*BPL) with Nucleoside-Based Bisubstrate Adenylation Inhibitors. *J. Med. Chem. 58*, 7349−7369.

(23) Sogi, K. M., Gartner, Z. J., Breidenbach, M. A., Appel, M. J., Schelle, M. W., and Bertozzi, C. R. (2013) *Mycobacterium tuberculosis* Rv3406 is a type II alkyl sulfatase capable of sulfate scavenging. *PLoS One 8*, e65080.

(24) Epp, J. B., and Widlanski, T. S. (1999) Facile Preparation of Nucleoside-5′-carboxylic Acids. *J. Org. Chem. 64*, 293−295.

(25) Gallo-Rodriguez, C., Ji, X.-d., Melman, N., Siegman, B. D., Sanders, L. H., Orlina, J., Fischer, B., Pu, Q., and Olah, M. E. (1994) Structure-Activity Relationships of N6-Benzyladenosine-5′-uronamides as A3-Selective Adenosine Agonists. *J. Med. Chem. 37*, 636−646.

(26) Okada, M., Iwashita, S., and Koizumi, N. (2000) Efficient general method for sulfamoylation of a hydroxyl group. *Tetrahedron Lett. 41*, 7047−7051.

(27) Bligh, C. M., Anzalone, L., Jung, Y. C., Zhang, Y., and Nugent, W. A. (2014) Preparation of both C5′ epimers of 5′-C-methyladenosine: reagent control trumps substrate control. *J. Org. Chem. 79*, 3238−3243.

(28) Somu, R. V., Boshoff, H., Qiao, C., Bennett, E. M., Barry, C. E., and Aldrich, C. C. (2006) Rationally Designed Nucleoside Antibiotics That Inhibit Siderophore Biosynthesis of Mycobacterium tuberculosis. *J. Med. Chem. 49*, 31−34.

(29) Velazquez-Campoy, A., and Freire, E. (2006) Isothermal titration calorimetry to determine association constants for high-affinity ligands. *Nat. Protoc. 1*, 186−191.

(30) Kovaleva, E. G., and Lipscomb, J. D. (2008) Versatility of biological non-heme Fe(II) centers in oxygen activation reactions. *Nat. Chem. Biol. 4*, 186−193.

(31) Lipscomb, J. D. (2008) Mechanism of extradiol aromatic ring-cleaving dioxygenases. *Curr. Opin. Struct. Biol. 18*, 644−649.

(32) Galvão, T. C., Lima, C. R., Gomes, L. H. F., Pagani, T. D., Ferreira, M. A., Gonçalves, A. S., Correa, P. R., Degrave, W. M., and Mendonça-Lima, L. (2014) The BCG Moreau RD16 deletion inactivates a repressor reshaping transcription of an adjacent gene. *Tuberculosis 94*, 26−33.

(33) Gopalan, A., Bhagavat, R., Chandra, N., Subbarao, S. H., Raja, A., and Bethunaickan, R. (2018) Biophysical and biochemical characterization of Rv3405c, a tetracycline repressor protein from *Mycobacterium tuberculosis*. *Biochem. Biophys. Res. Commun. 496*, 799−805.

(34) Schmidt, B., Selmer, T., Ingendoh, A., and von Figura, K. (1995) A novel amino acid modification in sulfatases that is defective in multiple sulfatase deficiency. *Cell 82*, 271−278.

(35) Bebrone, C. (2007) Metallo-beta-lactamases (classification, activity, genetic organization, structure, zinc coordination) and their superfamily. *Biochem. Pharmacol. 74*, 1686−1701.

(36) Diez-Roux, G., and Ballabio, A. (2005) Sulfatases and human disease. *Annu. Rev. Genomics Hum. Genet. 6*, 355−379.

(37) Hausinger, R. P. (2004) FeII/alpha-ketoglutarate-dependent hydroxylases and related enzymes. *Crit. Rev. Biochem. Mol. Biol. 39*, 21−68.

(38) Neres, J., Hartkoorn, R. C., Chiarelli, L. R., Gadupudi, R., Pasca, M. R., Mori, G., Venturelli, A., Savina, S., Makarov, V., Kolly, G. S., Molteni, E., Binda, C., Dhar, N., Ferrari, S., Brodin, P., Delorme, V., Landry, V., de Jesus Lopes Ribeiro, A. L., Farina, D., Saxena, P., Pojer, F., Carta, A., Luciani, R., Porta, A., Zanoni, G., De Rossi, E., Costi, M. P., Riccardi, G., and Cole, S. T. (2015) 2-Carboxyquinoxalines Kill *Mycobacterium tuberculosis* through Noncovalent Inhibition of DprE1. *ACS Chem. Biol. 10*, 705−714.

(39) Bolla, J. R., Do, S. V., Long, F., Dai, L., Su, C. C., Lei, H. T., Chen, X., Gerkey, J. E., Murphy, D. C., Rajashankar, K. R., Zhang, Q., and Yu, E. W. (2012) Structural and functional analysis of the

DOI: 10.1021/acsinfecdis.8b00038
ACS Infect. Dis. XXXX, XXX, XXX−XXX

transcriptional regulator Rv3066 of *Mycobacterium tuberculosis*. *Nucleic Acids Res. 40*, 9340−9355.

(40) Engohang-Ndong, J., Baillat, D., Aumercier, M., Bellefontaine, F., Besra, G. S., Locht, C., and Baulard, A. R. (2004) EthR, a repressor of the TetR/CamR family implicated in ethionamide resistance in mycobacteria, octamerizes cooperatively on its operator. *Mol. Microbiol. 51*, 175−188.

(41) Perrone, F., De Siena, B., Muscariello, L., Kendall, S. L., Waddell, S. J., and Sacco, M. (2017) A Novel TetR-Like Transcriptional Regulator Is Induced in Acid-Nitrosative Stress and Controls Expression of an Efflux Pump in Mycobacteria. *Front. Microbiol. 8*, 2039.

(42) Warrier, T., Kapilashrami, K., Argyrou, A., Ioerger, T. R., Little, D., Murphy, K. C., Nandakumar, M., Park, S., Gold, B., Mi, J., Zhang, T., Meiler, E., Rees, M., Somersan-Karakaya, S., Porras-De Francisco, E., Martinez-Hoyos, M., Burns-Huang, K., Roberts, J., Ling, Y., Rhee, K. Y., Mendoza-Losana, A., Luo, M., and Nathan, C. F. (2016) *N*-methylation of a bactericidal compound as a resistance mechanism in *Mycobacterium tuberculosis*. *Proc. Natl. Acad. Sci. U. S. A. 113*, E4523−4530.

(43) Jawalekar, A. M., Meeuwenoord, N., Cremers, J. S., Overkleeft, H. S., van der Marel, G. A., Rutjes, F. P., and van Delft, F. L. (2008) Conjugation of nucleosides and oligonucleotides by [3 + 2] cycloaddition. *J. Org. Chem. 73*, 287−290.

(44) Reuter, D. C., McIntosh, J. E., Guinn, A. C., and Madera, A. M. (2003) Synthesis of Vinyl Sulfonamides Using the Horner Reaction. *Synthesis 2003*, 2321−2324.

(45) Heacock, D., Forsyth, C. J., Shiba, K., and Musier-Forsyth, K. (1996) Synthesis and aminoacyl-tRNA synthetase inhibitory activity of prolyl adenylate analogs. *Bioorg. Chem. 24*, 273−289.

(46) Susumu, K., Uyeda, H. T., Medintz, I. L., Pons, T., Delehanty, J. B., and Mattoussi, H. (2007) Enhancing the stability and biological functionalities of quantum dots via compact multifunctional ligands. *J. Am. Chem. Soc. 129*, 13987−13996.

DOI: 10.1021/acsinfecdis.8b00038
ACS Infect. Dis. XXXX, XXX, XXX−XXX